Three interacting excitons in three coupled quantum dots

1998 J. Phys.: Condens. Matter 10 4335

(http://iopscience.iop.org/0953-8984/10/19/021)

J. Phys.: Condens. Matter **10** (1998) 4335–4352. Printed in the UK PII: S0953-8984(98)87682-0

Three interacting excitons in three coupled quantum dots

C Y Fong†, Barry M Klein†, L A Hemstreet‡, L H Yang§ and J S Nelson‖

† Department of Physics, University of California, Davis, CA 95616-8677, USA
‡ Code 6877, Naval Research Laboratory, Washington, DC 20375-5347, USA
§ Lawrence Livermore National Laboratory, Livermore, CA 94551, USA
‖ Semiconductor Physics Division, 1112, Sandia National Laboratories, Albuquerque, NM 87185-5800, USA

Received 17 September 1997, in final form 11 February 1998

Abstract. Using a scaled Kohn–Sham formalism, we examine *three* heavy- and light-hole excitons, respectively, in three coupled quantum dots to study the effects of competition involving the electron–electron and hole–hole interactions between excitons, the electron–hole interaction within excitons and the effective masses. The particle–particle interactions play dominant roles in determining the configuration of the excitons in the coupled dots. In the absence of an external electric field, the two lowest (occupied) energy states of the heavy-hole excitons are degenerate, and the excitons have an equal probability of residing in either of the two side dots. The corresponding states of the light-hole excitons exhibit nondegenerate character and the lowest energy exciton is confined predominantly to the centre dot. Under a weak dc electric field, both the heavy- and light-hole excitons form direct excitons which are localized in the side dots. For large values of the electric field, we find that the electrons associated with the excitons become ionized as a result of strong confinement by the field and the electron–electron repulsion between excitons before the excitons can be transformed into indirect excitons. This result is in contrast to the conclusion that a single exciton in a double-quantum-well structure will be transformed into an indirect exciton in real space when it is subjected to large fields. Furthermore, we suggest that the wave function overlap between interacting excitons may diminish significantly the increase in excitonic lifetime predicted for a single exciton in two coupled quantum dot systems, implying that it may be difficult to make use of several excitons in coupled structures for nonlinear devices.

1. Introduction

Excitons in nano-structures such as quantum wells, quantum wires and quantum dots (QDs), are expected to contribute significantly to future nonlinear optoelectronic applications [1]. The behaviour of excitons in such quantum structures differs from that in a bulk semiconductor due to the effects of confinement. The envelope functions for the electron and the hole of an exciton have to be subjected to additional boundary conditions imposed by the geometry of the quantum structure. This type of confinement for an exciton in a quantum dot has been studied by Einevoll [2] using parametrized Luttinger interactions [3] and by Que [4] with a parabolic confinement potential. Simple sine function forms of the envelope functions have been used by Barenco and Dupertuis [5] as basis functions for calculating matrix elements in their model Hamiltonian treatment of up to four excitons in a QD. However, only one kind of hole was considered. Furthermore, Coulomb interactions were treated in a perturbational sense.

More recently, Gotoh *et al* [6] have used similar basis functions to diagonalize the exciton effective mass Hamiltonian matrix and have calculated absorption spectra for an

0953-8984/98/194335+18$19.50

exciton in a rectangular box. Bryant [7] has used a variational approach to investigate the case of two excitons in a symmetric double-quantum-well structure and the ground state exciton in an asymmetric double-well structure, respectively, including both the effects of lateral confinement and an external dc electric field. Although most of his results were concerned with the ground state exciton, he pointed out that excitons can be transformed from direct to indirect excitons (in real space) as the magnitude of the electric field becomes large enough to overcome the Coulomb interaction between the electron and the hole. As the exciton is transformed from direct to indirect in a strong electric field, the recombination matrix element will be sharply reduced and an exciton with a long lifetime can exist and contribute to nonlinear optical properties for the excitonic system. Therefore, excitons in coupled quantum structures would appear to be interesting candidates for future nonlinear electronic device applications.

None of the above calculations, however, have seriously considered the interactions between excitons in a self-consistent manner. It is not clear, for example, how the various interactions and overlaps of the wave functions between excitons will affect features such as the excitonic lifetime which are important for nonlinear devices. To address such questions one needs a theoretical approach which goes beyond the existing treatment of the electron–hole (e–h) interaction employed by Bryant [7], which can become quite laborious as the number of excitons increases. Furthermore, one also would like to be able to treat the electron–electron (e–e) and hole–hole (h–h) interactions between excitons in a self-consistent way.

In this paper we extend a method used previously for investigating interacting electrons in confined quantum structures to treat the case of interacting excitons. Our approach is based on density functional theory [8] combined with the local density approximation (LDA) to exchange and correlation [9], and employs a scaled Kohn–Sham formalism [10, 11] so that all the particle–particle interactions are treated self-consistently within a single-particle framework. It has been applied successfully to treat several electrons in a quantum dot with a constriction [10], electronic tunnelling between quantum dots [11], donor states in coupled quantum dots [12] and the energy spacing of adding one electron at a time to a single dot [13]. In addition to the Coulomb interaction, the method includes both correlation and exchange (within the LDA) in the e–e and h–h interactions and, in this respect, differs from other approaches using Thomas–Fermi [14] and Hartree-exchange [15] density functionals. And because plane waves are used as basis functions, it is possible to manage difficult boundary conditions efficiently so that theoretical investigations can provide useful design information for interesting quantum structures as well as a microscopic description of the effects of the interactions.

The combination of the density functional method and the local density approximation has been used successfully to treat similar problems in a number of previous investigations. In addition to the references cited above, Wunsche and Henneberger [16] used density functional theory, including exchange and correlation within the LDA, to calculate the binding energies of localized few-particle complexes consisting of up to two excitons bound at a fixed Coulomb centre and obtained excellent agreement with elaborate variational calculations. They concluded that the LDA is an appropriate and sufficiently accurate tool for calculating the binding energies of such small complexes. Pfeiffer and Shore [17] used a similar approach to calculate the energetics of small exciton complexes bound to donors in silicon and germanium and obtained good agreement with experimental recombination spectra and exciton capture energies. Puls [18] *et al* employed the LDA to investigate the localization by alloy disorder of biexcitons in 5 nm thick II–VI quantum wells. They were able to obtain reasonably good agreement with experimental values of the biexciton

binding energies in a number of differently constructed (Zn,Cd)Se quantum wells and were able to demonstrate that the localized biexciton is a stable excitation of the disordered alloy potential. They also pointed out that the correlation energy in III–V quantum structures should be even smaller than in II–VI materials because of the difference in the static dielectric constants. All of these examples indicate that the combination of density functional theory with the LDA is an appropriate framework for investigating the energetics of systems with low particle density in confined geometries and should be well suited to treat the problem of interacting excitons in coupled quantum dots considered here.

In order to gain simple pictures for interacting excitons, we shall restrict our discussions in this paper to the case of three excitons in three coupled cubic QDs, so that two excitonic states are occupied in the ground state configuration of the system. If the states are nondegenerate, the lowest energy electron (hole) state is occupied by two electrons (holes) and the next higher energy electron (hole) state is singly occupied. The extra degree of freedom provided by using three coupled QDs instead of two is used to bring out the effects of the particle–particle interactions more clearly. To study the sensitivity of the excitonic properties to changes in boundary conditions (i.e. effective coupling between the QDs due to the effective masses) and applied electric fields, we shall discuss two heavy-hole exciton examples with different confinements as well as a light-hole exciton.

The paper is organized as follows: in section 2 we describe our models of the coupled quantum dots and we present a brief discussion of a logical way to introduce a self-consistent coupling between the electron and hole subsystems. This is followed by a discussion of our results for the energetics of interacting excitons without (section 3) and with (section 4) an external dc electric field, including some comments on the recombination matrix elements near the end of section 4. Finally, in section 5, a summary will be given.

2. Models and formalism

A rectangular supercell, indicated by the thick solid lines in figure 1, is used to model the system of three coupled quantum dots. The three cubic dots within each supercell are outlined by the thin lines. Each dot is assumed to be made of GaAs. There is a thick 4.0 nm wide barrier, which is labelled by b in figure 1, surrounding the three dots in each supercell. As we shall see later, this barrier separates effectively the three dots in one unit cell from those in neighbouring cells. There also are two identical thinner barriers of width 0.5 nm, labelled by d in figure 1, between the centre dot and the two side dots, respectively. All the barrier regions are assumed to be made of AlAs. Complications which occur in thin superlattices of GaAs/AlAs [19] due to the lowering of the conduction band state of AlAs at the X-point of the zinc-blende Brillouin zone are neglected. Because the conduction and valence band discontinuities for a GaAs/AlAs heterostructure are different, the barrier heights for the electron and the hole will have different values. The parameters used in our calculations are summarized in table 1. We choose our reference potential such that the potential in the barrier regions is set equal to zero. Then, the dot regions will have different negative potentials for electrons and holes, respectively.

To examine the competition between the particle–particle interactions and the effects of confinement, we consider two different sizes of QDs for the heavy-hole excitons but keep all the barrier widths constant. We vary the dot size only for the heavy-hole excitons because of the large effective mass of the heavy hole as compared to that of the electron (table 1). By contrast, the light-hole mass is of the same order of magnitude as the electron effective mass and the effects of confinement on the light-hole excitons can simply be deduced from the electron case [12]. The cubic edges for the two sizes of QDs used in the heavy-hole

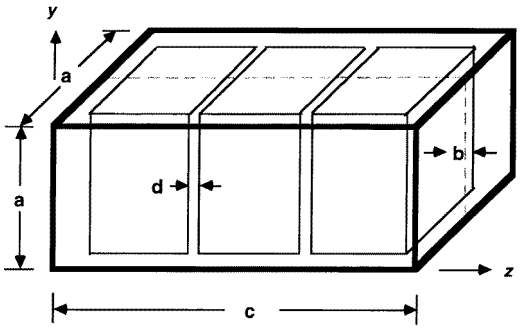

Figure 1. The supercell model of three coupled quantum dots.

Table 1. The parameters characterizing the model calculations.

	Effective mass m^{*a}	Barrier height V_{ext} (meV)	Dielectric constant ε
Electron	0.067	899.8 [24]	
Heavy hole	0.377	544.0 [24]	10.0
Light hole	0.082		

[a] in units of the free electron mass.

exciton studies are chosen to be 23.8 nm and 18.5 nm, respectively. Accordingly, the lattice parameters for the supercell with the larger QDs are 31.8 nm along the $\boldsymbol{x}$ and $\boldsymbol{y}$ directions (labelled by a in figure 1) and 80.4 nm along the $\boldsymbol{z}$ direction (labelled by c), while the corresponding parameters for the supercell containing the smaller dots are 26.5 nm and 64.5 nm, respectively.

The Kohn–Sham formalism [9] has been extended to multicomponent systems by Kohn and Vashishta [20]. Following the derivations given in [20], the ground state properties of the excitonic system can be determined by solving two coupled sets of Kohn–Sham equations for an electron and a hole, respectively:

$$\left\{\left(-\hbar^2/2m_e^*\right)\nabla^2 + V_{ext}\left(\boldsymbol{r}_e\right) + V_{e-e}\left(\boldsymbol{r}_e, [\rho_e]\right) + V_{h-e}\left(\boldsymbol{r}_e - \boldsymbol{r}_h, [\rho_h]\right)\right\}\Psi_e\left(\boldsymbol{r}_e\right) = E_e\Psi_e\left(\boldsymbol{r}_e\right) \tag{1}$$

$$\Sigma_l \left|\Psi_{el}\left(\boldsymbol{r}_e\right)\right|^2 = \rho_e\left(\boldsymbol{r}_e\right) \tag{2}$$

and

$$\left\{\left(-h^2/2m_h^*\right)\nabla^2 + V_{ext}\left(\boldsymbol{r}_h\right) + V_{h-h}\left(\boldsymbol{r}_h, [\rho_h]\right) + V_{e-h}\left(\boldsymbol{r}_h - \boldsymbol{r}_e, [\rho_e]\right)\right\}\Psi_h\left(\boldsymbol{r}_h\right) = E_h\Psi_h\left(\boldsymbol{r}_h\right) \tag{3}$$

$$\Sigma_{l'} \left|\Psi_{hl'}\left(\boldsymbol{r}_h\right)\right|^2 = \rho_h\left(\boldsymbol{r}_h\right). \tag{4}$$

In these equations, $V_{ext}(\boldsymbol{r}_e)$ (in (1)) and $V_{ext}(\boldsymbol{r}_h)$ (in (3)) are the potentials defining the dot regions and the external dc electric field acting on the electron and the hole, respectively, m_e^* and m_h^* are the effective masses of the electron and the hole, and $V_{e-e}(\boldsymbol{r}_e, [\rho_e])$ (in (1)) and $V_{h-h}(\boldsymbol{r}_h, [\rho_h])$ (in (3)) are the potential functions characterizing the e–e and h–h interactions, including exchange and correlation in the form of Ceperley and Alder [21] as parametrized

by Perdew and Zunger [22]. The summations over l and l' in (2) and (4) are over the occupied states of the electrons and holes, respectively. The terms $V_{h-e}(\boldsymbol{r}_e - \boldsymbol{r}_h, [\rho_h])$ (in (1)) and $V_{e-h}(\boldsymbol{r}_h - \boldsymbol{r}_e, [\rho_e])$ (in (3)) are the potential functions for the hole–electron (h–e) and e–h interactions acting on an electron and a hole, respectively. They provide the coupling between the electron and the hole subsystems, as the former depends on the hole density, ρ_h, and the latter depends on the electron density, ρ_e. For the present calculations, we consider *only* the Coulomb interaction between electrons and holes and refer to both of these potentials as simply 'the e–h interaction' in later discussions. These terms, as well as the e–e and h–h interactions, are screened by the dielectric constant, ε, of the dot. As shown in [11], if one measures the effective masses in units of 0.1 of the free electron mass, m_0, lengths in units of 10 nm and V_{ext} in units of meV, then the length (nm) and energy scales (meV) in (1) and (3) are consistent with those of laboratory grown samples and measurements.

We have used the following self-consistent procedure for solving the coupled equations. Initially neglecting the e–h interaction, we (a) solve self-consistently (1) and (2) for the electron, and (3) and (4) for the hole; (b) then we use the electron and the hole charge densities obtained in (a) to construct the e–h interaction potential for the hole and for the electron, respectively, thereby coupling the electron and the hole subsystems; (c) finally we repeat steps (a) and (b) until all the particle–particle interactions in the coupled systems are self-consistent. The results of step (a) are, in fact, those of the confined free electron and hole states that will be discussed later on in section 3.

Plane waves are used as basis functions in our calculations. The number of plane waves in the basis set has been determined by the convergence of the eigenvalues of the electron and hole subsystems. We have chosen 1.2×10^3 meV as the plane wave kinetic energy cutoff for the heavy-hole excitons in the larger dots, which results in a basis set containing more than 7500 plane waves. For the light-hole excitons in the larger dots, the cutoff energy is taken to be 1.1×10^3 meV and there are about 6300 plane waves available to approximate the wave functions. The maximum kinetic energy is increased to 1.6×10^3 meV when the smaller dots are used to assess the effects of confinement on the heavy-hole excitons. This choice results in more than 6700 plane waves. With these kinetic energy cutoffs, all energy levels are converged to within the order of 0.01 meV. The eigenvalues have been calculated using the relaxation method of Woodward *et al* [23].

3. Interacting excitons in the absence of an external field

In this section, we shall first present results for the energetics of the heavy- and light-hole excitons in the absence of an external dc electric field. Because of the symmetry possessed by the three coupled cubic QDs, the electron and hole states can be classified as either symmetric (even) or antisymmetric (odd) with respect to the z direction (figure 1), as discussed in [7]. For simplicity, we shall focus only on excitons formed by combinations of even or odd electron and hole states, respectively, where the nature of the states is identified from the symmetry properties of the wave functions. The former will be called even state excitons while the latter will be termed odd state excitons. We shall not consider any mixed state excitons with an even parity electronic state and an odd parity hole state, or vice versa. As we shall see later, the definition of the 'binding energy' of a pure even or odd state exciton can be ambiguous in the presence of an external potential. Consequently, we shall use the term 'energy difference' to define the energy of an exciton. This quantity is simply the sum of the energy differences of the electron and the hole measured with respect to their respective reference energies, which have been calculated without e–h interactions and

without an external field. Our choice of reference states for the electrons and holes will be described in section 3.1. This will be followed by a discussion of the energetics of the heavy-hole excitons, including the effects of confinement, in 3.2. This section will conclude with a presentation of our results for the light-hole excitons in 3.3.

3.1. Reference states for electrons and holes

It is well known that LDA calculations severely underestimate the fundamental energy gaps of semiconductors. We, therefore, need a proper reference energy other than the LDA gap energy in order to define the energy of an exciton. We have adopted an approach analagous to that used in [12] for the donor problem, where the binding energy of the donor electron was defined as the energy difference without (as a reference) and with the ion–electron interaction. For each exciton, the reference energy for the electron, denoted by E_c, is taken to be the lowest occupied electronic state of three interacting electrons in the same supercell as the exciton but without the e–h interaction. We denote the electrons in this hole-free system as 'confined free electrons'. Similarly, the three interacting holes in the supercell without electrons ($V_{e-h} = 0$) are called 'confined free holes', and the energy of the highest occupied hole state, labelled by E_v, will serve as the reference energy for the holes.

The relevant energy levels for a system composed of three 'confined free electrons' and three 'confined free holes' (i.e., neglecting electron–hole interactions) are schematically shown on the left-hand side (LHS) of figure 2(a). The reference energies for measuring the energies of the excitons are labelled by E_c and E_v, respectively. Note that there is a splitting of 0.74 meV between the lowest (even) and the next higher energy (odd) electronic states, while the corresponding hole states are degenerate. This difference between the two reference subsystems is the result of the competition between the effective masses and the particle–particle interactions, as we shall now discuss.

First consider the 'confined free electron' case. When the dots are infinitely far apart, or when the barriers between the dots are large or thick enough to completely isolate the dots from each other, each dot will have an s-like lowest energy state whose wave function does not exhibit any nodes in the dot [12]. With $d = 0.5$ nm barriers between the dots, these electron states will couple due to the small effective mass ($0.067\ m_0$) of the electrons, and the three s-like states will form three linearly combined states for the coupled system. The charge density of the resulting ground state in a (100) section passing through the centre of the supercell (outlined by the dashed section in figure 1) is plotted in figure 2(b). Note that this ground state is doubly occupied because of spin degeneracy. In this plot, the interval between the contours is determined by dividing the maximum and minimum values into 15 levels and the maximum charge density (including the weighting factor of the occupancy of the state) is given in the figure caption (this same format will be used for all the charge density plots presented in this paper). The charge distribution in figure 2(b) is symmetric in the coupled, z, direction to be consistent with the symmetry of the QD system, and is spread out among the three dots due to the electron coupling. The maximum of the charge density ($29.58 \times 10^{-5}\ e\ \mathrm{nm}^{-3}$) is located at the centre of the middle dot. The associated secondary maxima in the two side dots are each about 64% ($18.94 \times 10^{-5}\ e\ \mathrm{nm}^{-3}$) of the absolute maximum. This result suggests that this linear combination is formed by the s-like states in the individual dots but is modulated by a sinelike function to satisfy the boundary condition imposed by the thicker barrier, b. The spreading of the wave function throughout the dots minimizes the kinetic energy of the system. By examining the expansion coefficients of the wave function onto the plane wave basis functions, we find that this state has even parity with respect to the z direction. This state is labelled as 'even' in figure 2(a) and serves as

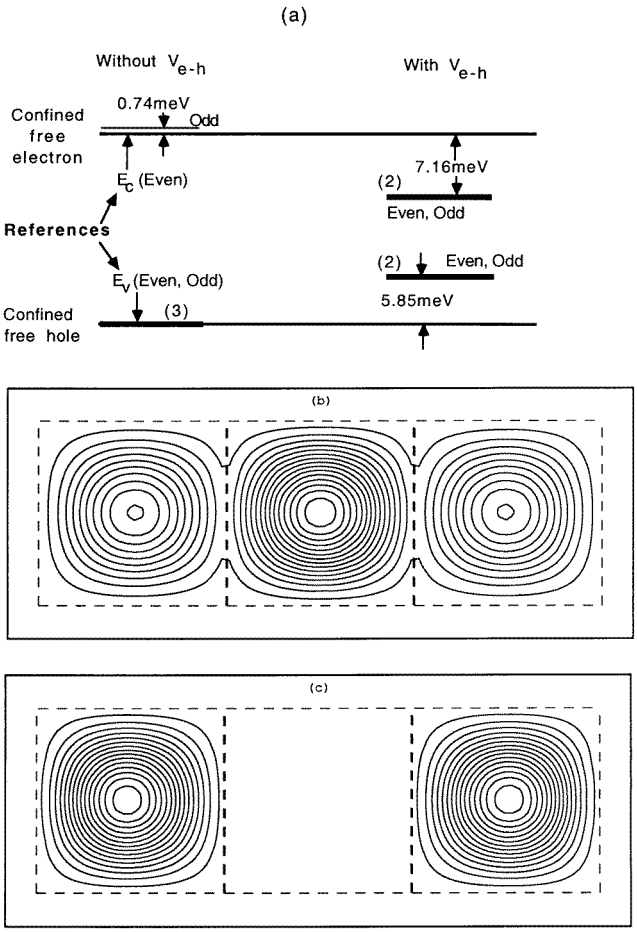

Figure 2. (a) Schematic diagram of the energy differences, ΔE, of the heavy-hole excitons in the larger quantum dots (light lines for the electrons, and heavy lines for the holes) without ΔV. The charge distributions of the confined free electron states with (b) even parity (maximum at centre is 29.58×10^{-5} e nm^{-3}) and (c) odd parity (maximum: 17.78×10^{-5} e nm^{-3}).

the electronic reference level (E_c) for determining the energy of the excitons.

The next higher energy state is only singly occupied in the case of three electrons and has its charge density localized in the side dots with essentially no charge in the centre dot, as shown in figure 2(c). The wave function of this first excited state, labelled 'odd' in figure 2(a), exhibits odd parity with respect to the coupled (z) direction of the dots. The maximum charge density of this odd electron state is only 60% of the value for the even state due to the inclusion of different occupancies for the two states in calculating the charge densities. The equal distribution of density in the two side dots shown in figure 2(c) is interpreted as implying an equal probability of finding the higher energy odd electron in either one of the side dots and is a consequence of minimizing the Coulomb repulsive part of the e–e interaction between the three electrons in the system. Since the two electrons occupying the ground state have a higher probability of being in the centre dot, the electron occupying the next higher energy state then will be pushed away from the centre dot into one of the side dots. The consequence of the Coulomb repulsion between the electrons, then, is

the splitting of the degeneracy of the two lowest lying occupied states. We note in passing that the charge density plots in figures 2(b) and (c) show clearly that the thick barrier, b, effectively decouples the three dots in one supercell from those in the neighbouring cells.

The heavy-hole mass is about 5.6 times larger than the electron mass (table 1) and causes the effective heavy-hole coupling between the dots to be significantly reduced in comparison to the electron case. Therefore, the three s-like heavy-hole states remain practically degenerate even as the barrier width between the dots is reduced to the small value of d used here (the energy difference between the two occupied states and the unoccupied state remains less than 0.002 meV). The charge densities of the two occupied states (not shown) are qualitatively similar to the ones shown in figure 2(b) and (c). However, the maximum charge density of the even heavy-hole state in the centre dot (15×10^{-5} e nm^{-3}) and its secondary maxima in the two side dots (13.52×10^{-5} e nm^{-3}) are comparable in magnitude and do not exhibit any modulation behaviour as in the electron case. This even heavy-hole state is, therefore, a simple linear combination of the s-like states in each dot, with proper normalization. The other occupied state has an equal weighting factor and has charge density maxima with magnitude (16.89×10^{-5} e nm^{-3}) comparable to that of the even hole state located in each of the side dots. The reduction of the effective heavy-hole coupling between dots can be further demonstrated by comparing the charge densities of the occupied hole states in the barrier regions between the dots to the corresponding results for the electrons. For the heavy holes, the even state has a maximum charge density of 0.25×10^{-5} e nm^{-3} in the barrier and the odd state has a value of 5.0×10^{-8} e nm^{-3}. The corresponding values for the electron case are 2.19×10^{-5} and 0.26×10^{-5} e nm^{-3}, respectively, indicating that the coupling strengths for the heavy-hole states are definitely weaker than those of the electron states. The energy of the degenerate heavy-hole states will serve as the reference energy for determining the energy of the heavy-hole states of the excitons and is indicated by the thick line (labelled E_v) on the LHS of figure 2(a), with the degeneracy of the level shown in the parentheses.

3.2. Heavy-hole excitons

When the e–h interaction is switched on, the even and odd parity states of the electrons become nearly degenerate, as shown on the right-hand side (RHS) of figure 2(a), and are located 7.16 meV below their reference. The previously degenerate hole states, on the other hand, show some indication of splitting. The two occupied hole states, which experience the e–h interaction, remain degenerate but split off from the third (unoccupied) state and move up into the gap region by 5.85 meV with respect to their reference. As a result, the magnitude of the energy difference, ΔE, is the same (13.01 meV) for each of the two excitons formed by either the even parity electron and hole states or the odd parity electron and hole states, respectively.

In figures 3(a) to (d), we plot the heavy-hole and the corresponding electron charge densities for both the even (figures 3(a) and (b)) and the odd (figures 3(c) and (d)) state excitons. The two sets of plots are very similar. We note that neither excitonic state has its electronic charge concentrated in the centre dot, as was the case for the ground state of the 'confined free electrons'. We interpret these results as implying an equal probability of finding the even and odd state excitons in opposite side dots. This result is a consequence of the carriers' masses and the carrier–carrier interactions between the excitons. If the exciton were to have its hole charge located at the centre dot, its electron would tend to be in the centre dot as well because of the e–h interaction. However, the electronic charge would not localize completely within the centre dot, but would spread symmetrically into the side

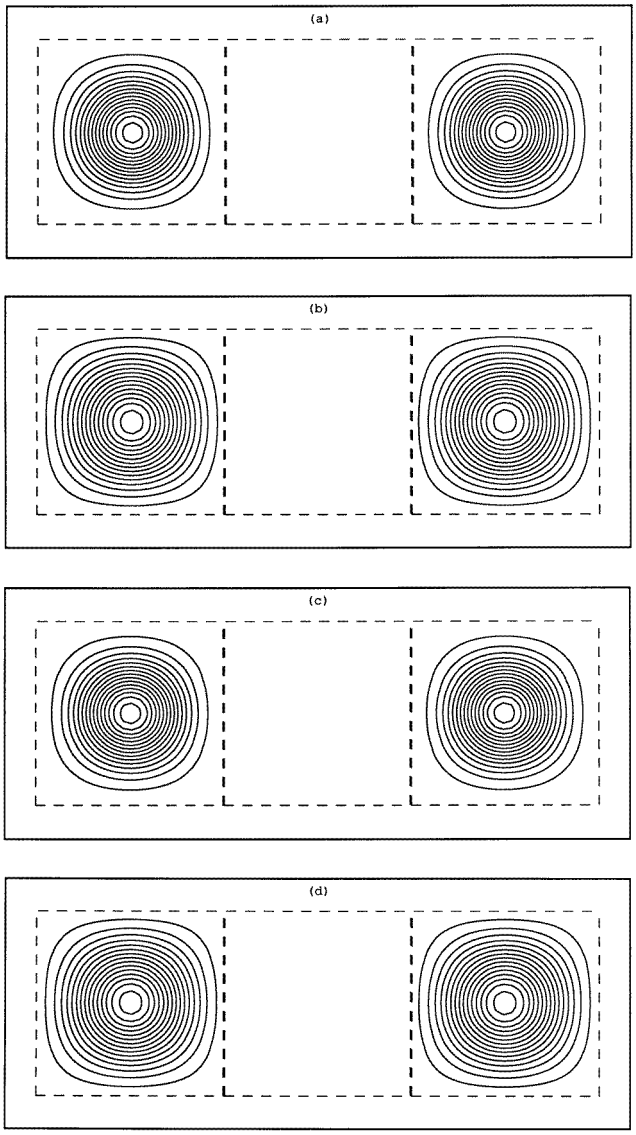

Figure 3. Charge distributions of the heavy-hole excitons: (a) the even heavy-hole state (maximum: 46.8×10^{-5} e nm^{-3}); (b) the even electron state (maximum: 34.74×10^{-5} e nm^{-3}); (c) the odd heavy-hole state (maximum: 46.8×10^{-5} e nm^{-3}) and (d) the odd electron state (maximum: 31.61×10^{-5} e nm^{-3}).

dots due to its light mass, similar to the situation shown in figure 2(b). Because of this spread, the e–h interaction would be reduced and the repulsive e–e interactions with the odd state exciton, which has equal probability of being in either of the side dots, would be stronger. In order to have the lowest ground state energy of the coupled system, the two lowest energy excitons thus are equally likely to reside in opposite side dots, as indicated in figure 3, in order to maximize the e–h interaction for each excitonic state as well as to reduce the e–e and h–h repulsions between the excitons by being as far apart as possible.

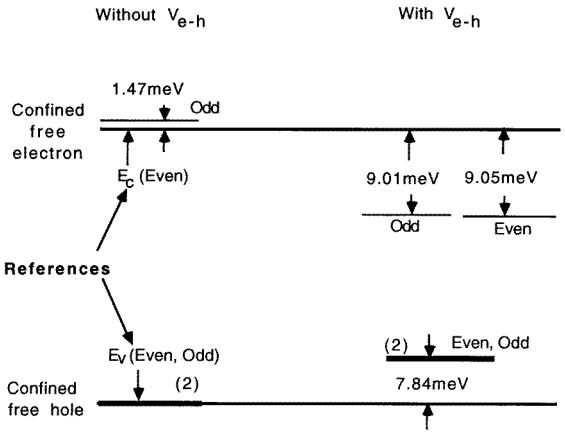

Figure 4. Schematic diagram of ΔE of the heavy-hole excitons in the smaller quantum dots (light lines for the electrons, and heavy lines for the holes) without ΔV.

To investigate the effect of confinement on the heavy-hole excitons, we have performed similar calculations for the heavy-hole excitons in smaller dots of size $18.5\times18.5\times18.5$ nm^3. Each dot comprises only 47% of the volume of the larger dots used previously. The schematic energy diagram is shown in figure 4. The corresponding reference energies for the electron and the hole again are labelled E_c and E_v, respectively. These energies do not have the same values as those shown in figure 2(a), however, because of the smaller size of the dots. Since an absolute reference energy for the two different sized dots is difficult to define, we use the individual references. Even so, we still can see the effects of greater confinement, particularly in the case of the electrons.

The splitting between the lowest and the next higher energy state of the 'confined free electrons' (LHS of figure 4) is now 1.47 meV, about twice as large as the value obtained for the larger dots. For the 'confined free holes', the large effective mass of the heavy hole continues to play a dominant role, but now the three linearly combined s-like hole states show a small splitting of 0.03 meV, which is essentially the limit of convergence for the eigenvalues. For simplicity, we show only the two highest energy heavy-hole states (indicated by the thick line on the LHS of figure 4) and consider them still to be degenerate (with the degeneracy specified by the number in parentheses). The increase in kinetic energy of the heavy-hole states due to their greater confinement is just beginning to induce significant coupling between the dots. This suggests that our calculations can determine the critical GaAs dot size and AlAs barrier width required for the heavy-hole states to interact.

As was the case with the larger dots, the e–h interaction pushes the energies of the electron and the hole states into the gap region defined by E_c and E_v. The ΔE values for the even and odd state excitons are calculated to be 16.89 meV and 16.85 meV, respectively. Both energies are greater than those obtained for the bigger dots (shown in figure 2(a)), indicating that the stronger Coulomb attraction between the electron and hole in the smaller dots overcomes the increase in kinetic energy due to the greater confinement of the electrons.

3.3. Light-hole excitons

We close this section with a presentation of our results for three light-hole excitons in the larger dot system. On the LHS of figure 5, we indicate the reference energies, E_c and E_v,

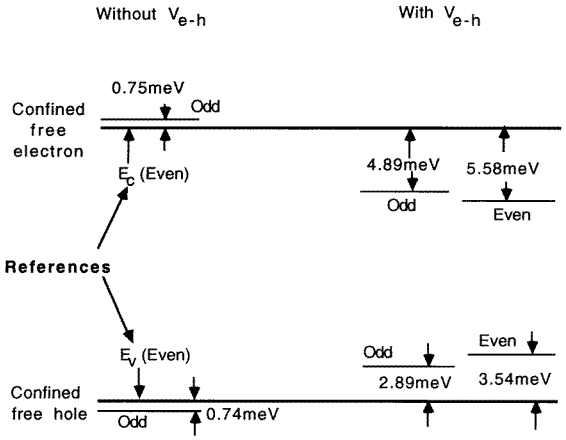

Figure 5. Schematic diagram of the ΔE of the light-hole excitons (light lines for the electrons, and heavy lines for the holes) without ΔV.

for the light-hole excitons. In fact, E_c is the same as shown in figure 2(a). Without the e–h interaction, the even and odd parity states of both electrons and holes are separated in energy because of the coupling between dots which results from their small masses (the light-hole coupling is stronger—the electron coupling is the same as before). The charge distributions of the two highest energy light-hole states (not shown) are similar to those of the confined free electrons shown in figures 2(b) and 2(c), with the even parity state of the light hole centred on the middle dot but having its charge spread out over all three dots.

With the e–h interaction included, the energy differences of the even and odd state excitons are calculated to be 9.12 and 7.68 meV, respectively. These values are smaller than those obtained for the heavy-hole excitons and can be attributed to the fact that the light-hole excitons are less localized in the coupled QDs. More evidence for stronger light-hole coupling between the dots can be provided by the charge densities. The contour plots of the charge densities for the hole and electron states of the even state exciton are given in figures 6(a) and 6(b). The contours for the odd state exciton are not shown; they are localized in the two side dots and are similar to those shown in figure 2(c). Comparison of figure 6 to the corresponding results obtained for the even state heavy-hole exciton (figures 3(a) and 3(b)) indicates that the charge distributions of both the electron and hole of the even state light-hole exciton are spread out over the entire coupled dot system instead of being localized in the side dots, as was the case for the heavy-hole exciton. In fact, the light-hole state (figure 6(a)) looks very much like the even parity confined free electron state (figure 2(b)), and the light-hole charge density in the barrier region is of the same order of magnitude as that of the confined free electron state. The kinetic energy of the even state exciton is lower than that of the odd state exciton because of the spread of both the even parity electron and hole wave functions, so that the even state exciton becomes the lowest energy state of the light-hole excitons. This stands in contrast to the degenerate heavy-hole result. These results demonstrate that competition between the e–e interaction, the h–h interaction, the e–h interaction and the effective masses determines the most probable locations for finding the even and odd state excitons in a coupled three QD system without an external field.

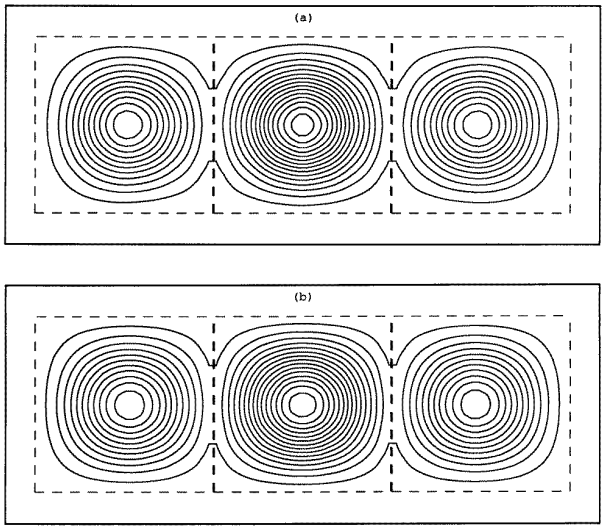

Figure 6. Charge distributions of the even light-hole excitons: (a) the even light-hole state (maximum: 34.89×10^{-5} e nm^{-3}), and (b) the even electron state (maximum: 31.54×10^{-5} e nm^{-3}).

4. Interacting excitons in an external dc electric field

Now we shall discuss the energy differences, ΔE, of the excitons as functions of an external potential, ΔV, which is used to simulate an externally applied dc electric field across the three dots. Because ΔV is increased gradually, we are able to identify the electron and the hole wave functions derived from the even and odd parity states even though the parity symmetry is broken by ΔV. Therefore, we shall continue to use the terms *even* and *odd* to characterize the excitonic states in the presence of an external field.

When the left edge of the LHS dot in figure 1 is raised (for electrons) by an external potential, ΔV, one expects that the electron and the hole will move in opposite directions (the electron moves to the right, along the z direction of figure 1, while the hole moves to the left). It has been demonstrated by Bryant [7] that a single direct exciton in a double-well system will be transformed into an indirect exciton in the presence of an external electric field. Here we consider three excitons in a coupled QD system and we are interested in investigating the effects of the competition between the external field, the carrier–carrier interactions between excitons and the e–h interaction within an exciton in order to answer the question posed in the introduction: how do the various carrier–carrier interactions affect the excitonic properties of the coupled QD system in an external dc electric field? As we shall see, the carrier–carrier interactions can dominate and can change some of the conclusions deduced from the study of a single exciton. We shall discuss the energetics of three heavy-hole excitons in the presence of an electric field in section 4.1, and will include some comments on the recombination matrix elements. We shall conclude the section with a brief summary of the light-hole results in 4.2.

4.1. Heavy-hole excitons

In figure 7, we plot calculated energy differences for the even and odd state heavy-hole excitons as functions of ΔV using the same reference energies as shown in figure 2. As

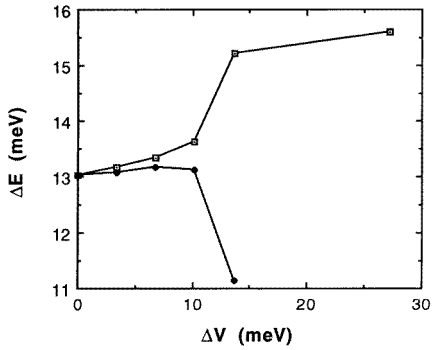

Figure 7. ΔE of the heavy-hole excitons against ΔV. Even state exciton (open squares), odd state exciton (filled diamonds).

mentioned earlier, we can follow the evolution of the even and odd states as the external potential is applied and so we shall continue to use the terms 'even' and 'odd' to characterize the excitonic states even though the parity symmetry is broken by ΔV. Results for the even state exciton are indicated by the curve with open squares while those for the odd state exciton are denoted by filled diamonds. For $\Delta V = 10.2$ meV, the most obvious effect of the field is to lift the degeneracy between the even and odd state excitons, with the odd state exciton having a smaller ΔE. At $\Delta V = 13.6$ meV, the energy of the odd state exciton decreases sharply, while the energy of the even state exciton still increases. After that, ΔE for the even exciton shows saturation. In fact, we should plot the results for the even state only up to 13.6 meV. We include the data for $\Delta V = 27.2$ meV simply to bring up a point about the ambiguity in defining a 'binding energy' for pure even and odd excitons, which will be discussed later.

Because of the initial degeneracy, it is difficult to see *a priori* why the even state exciton should have larger ΔE when there is an external field. We find that the electron of the even state exciton responds more sensitively to the field as ΔV is increased than does the electron associated with the odd state exciton. The charge density of this even electron state is concentrated more in the RHS dot where the potential of the electric field is the lowest. This is sufficient to cause the electronic part of the energy of this even state exciton to split off from the odd state exciton. As soon as the degeneracy is lifted, the occupancies of the states change. The lower energy state of the even state exciton is weighted more because three excitons are considered. The charge density of the even electron (hole) state, therefore, contributes more to the e–h interaction. Consequently, the odd state exciton experiences a weaker e–h interaction.

The behaviour of ΔE in figure 7 can be understood in terms of competition between the external field and the particle–particle interactions. We illustrate the competition by examining the charge distributions with finite ΔV. As the electronic charge of the even state exciton shifts to the RHS dot, the associated heavy-hole charge would be expected to move to the LHS dot under the influence of the electric field. However, for small fields, the stronger e–h interaction causes the hole charge distribution to remain localized in the same (RHS) dot as the electron, as shown in figures 8(a) and (b) for $\Delta V = 10.2$ meV. To minimize the Coulomb repulsion between the electrons and holes of the excitons, the odd state exciton is forced into the LHS dot, as shown in figures 8(c) and (d) for the hole and electron, respectively. The competition between the field and the e–h interaction can be seen easily in these plots because the densities are not completely confined to one of

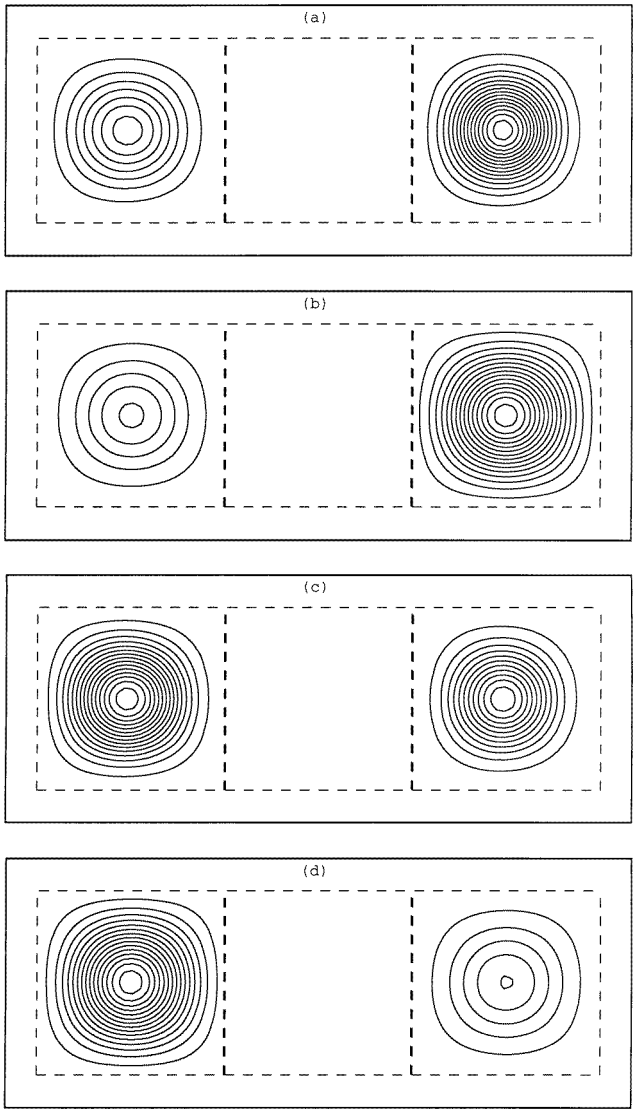

Figure 8. Charge distributions of (a) the heavy hole (maximum: 68.34×10^{-5} e nm^{-3}) and (b) the electron of the even state exciton (maximum: 61.62×10^{-5} e nm^{-3}); (c) the heavy hole (maximum: 50.25×10^{-5} e nm^{-3}) and (d) the electron (maximum: 34.11×10^{-5} e nm^{-3}) of the odd state exciton for $\Delta V = 10.2$ meV.

the side dots. However, by considering the locations of the major portions of the charge distributions, both excitons can be identified to be direct.

As ΔV is increased to 13.6 meV, the stronger electric field localizes the electronic charge density of the even state exciton even further into the RHS dot (the contours in the LHS dot of figure 8(b) are forced out) and the e–h interaction continues to pull the corresponding hole charge along with it, increasing ΔE for the even exciton. On the other hand, the e–e repulsion between the even and odd state excitons forces the electron of the odd state exciton to be localized completely within the LHS dot (the contours at the

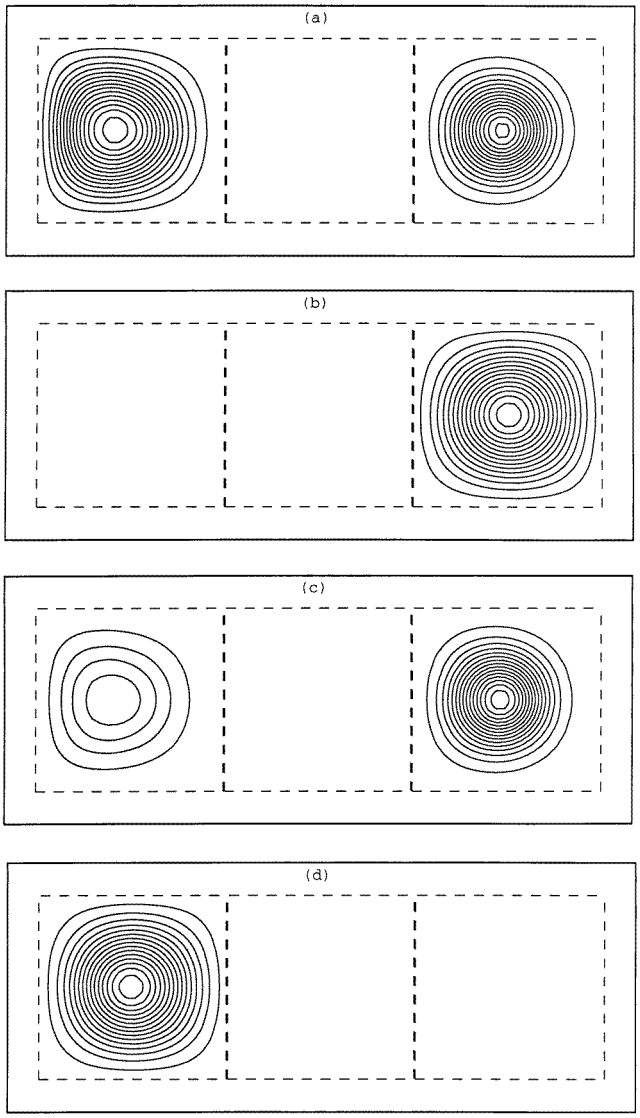

Figure 9. Charge distributions of (a) the heavy hole (maximum: 54.71×10^{-5} e nm^{-3}) and (b) the electron (maximum: 83.83×10^{-5} e nm^{-3}) of the even state exciton; (c) the heavy hole (maximum: 61.82×10^{-5} e nm^{-3}) and (d) the electron (maximum: 44.77×10^{-5} e nm^{-3}) of the odd state exciton for $\Delta V = 27.2$ meV.

RHS dot of figure 8(d) disappear). The combination of greater confinement, weaker e–h interaction and higher potential (close to ΔV) causes the electronic energy of the odd state exciton to be higher than the electronic reference energy. This result can be interpreted as the ionization of the odd state electron. Therefore, our results suggest that the electron of the odd state exciton will be ionized before the odd exciton has a chance to become an indirect exciton in real space.

As ΔV increases to 27.2 meV, the field strength becomes strong enough to overcome the e–h attraction for the even state exciton. The electron stays in the RHS dot while

the hole charge starts to shift from the RHS dot to the LHS dot as shown in figures 9(b) and (a), respectively. Due to the reduction of the e–h interaction between the electron and hole as they separate and the greater confinement of the electron by the external field, the electronic energy of the even state exciton increases and also becomes higher than the electronic reference energy, suggesting that the electron of the even state exciton also will be ionized before the exciton can become indirect.

Furthermore, the hole (electron) of the even state exciton now exerts a Coulomb repulsion on the hole (electron) state of the higher lying odd exciton and forces the odd state hole (electron) into the RHS (LHS) dot. The corresponding charge densities are shown in figures 9(c) and (d) for the odd state hole and electron, respectively. Because the higher energy odd state electron has already been ionized at this point, we do not label this pair as an indirect odd state exciton. The presence of the higher energy odd electron (hole) state in the same dot with the even hole (electron) state compensates for the reduction in ΔE of the even state exciton as its hole and electron are pulled apart by the field. This explains the saturation of ΔE for values of ΔV between 13.6 and 27.2 meV and is the source of ambiguity in defining the binding energy for the pure even and odd state excitons. In addition, the large overlap of the wave functions can result in a sizeable contribution (10^{-4} nm^{-2}) to the square of the dipole matrix element (i.e., the square of the matrix element of the gradient operator) which is the same order of magnitude as the recombination matrix element, as shown in the next paragraph. Therefore, it can be difficult for either the even or the odd state exciton to sustain a long lifetime under a large field because of this overlap.

As for the recombination matrix elements (the same as the matrix elements of the gradient operator) of the even and odd state excitons, we do not expect them to decrease sharply as ΔV increases because the excitons remain direct. This result is verified by our calculations. Due to the symmetry and dimensions in the $\boldsymbol{x}$, $\boldsymbol{y}$ and $\boldsymbol{z}$ directions of the QD system, the squares of the recombination matrix elements in the $\boldsymbol{x}$ and $\boldsymbol{y}$ directions are essentially zero (10^{-10} nm^{-2}), while the squared matrix element in the $\boldsymbol{z}$ direction is calculated to be of the order of 10^{-4} nm^{-2}).

4.2. Light-hole excitons

The corresponding results for ΔE as functions of ΔV for the even and odd state light-hole excitons are shown in figure 10. The qualitative features of both the even and odd state light-hole excitons under an external dc electric field are similar to those of the heavy-hole exciton. For small values of ΔV, the e–h interaction is still stronger than the field and both excitons are direct, with the charge distributions of the even state exciton concentrated more in the RHS dot while those for the odd state exciton are more localized in the LHS dot. There are, however, quantitative differences between the heavy- and the light-hole excitons. The smaller masses of the carriers cause the electron of the odd state light-hole exciton to be ionized at a smaller value of ΔV ($\sim$10.2 meV) than for the heavy-hole exciton ($\sim$13.6 meV), and the electron of the even light-hole exciton is ionized at 17 meV as compared to the value of 27.2 meV for the even heavy-hole case.

5. Summary

We have investigated three heavy- and light-hole excitons, respectively, in three coupled quantum dots to study the effects of the confinement and the competition between the e–e and h–h interactions between excitons, the e–h interaction within excitons and the effective

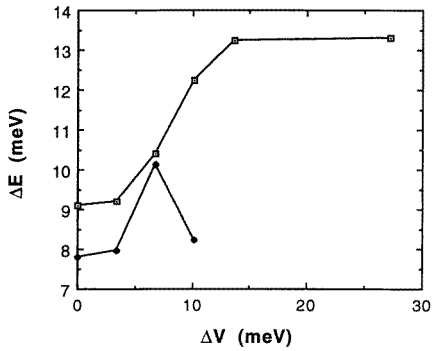

Figure 10. ΔE of the light-hole excitons against ΔV. Even state exciton (open squares), odd state exciton (filled diamonds).

masses. The scaled Kohn–Sham formalism has been used to treat, self-consistently, all of the e–e and h–h interactions. Only the Coulomb part of the interaction between the electron and the hole within an exciton has been considered

At zero external dc electric field, the effective mass difference between the heavy and the light holes and the particle–particle interactions cause the even and odd heavy-hole excitons to be degenerate in energy and to have equal probability of being found in either of the two side dots. The two light-hole exciton states, however, are nondegenerate in energy and the lowest energy (even state) exciton is confined to the middle dot. The next higher energy exciton has equal probability of residing in either of the side dots.

When the field is weak, the e–h interaction within the excitons dominates and both the heavy- and light-hole ground state excitons are localized more in the RHS dot where the electron of the even state exciton experiences the lowest potential of the field. The higher energy odd state excitons have both their electron and hole wave functions confined to the other side dot because of the Coulomb repulsion from the electrons and holes associated with the even exciton. Both the even and odd excitons are direct. These results agree with those obtained from the study of a single exciton in a system with two coupled QDs [7].

As the field increases, the electrons of the excitons (both heavy and light hole) are ionized before the excitons are transformed to indirect excitons. In addition, because of the e–e and h–h interactions between the excitons, the hole (electron) wave function of the even state exciton and the electron (hole) wave function of the odd state exciton can be localized in the same dot, causing an ambiguity for defining the binding energy of a pure even or odd exciton. Furthermore, the overlapping of these wave functions can facilitate the recombination process. Therefore, the lifetime of the excitons can be reduced significantly. All these results differ from the predictions based on the consideration of a single exciton. Our calculations suggest that, in practice, it may be difficult to make use of several excitons in a coupled array of QDs for nonlinear devices.

Acknowledgment

We thank Z W Lu, John Pask and C Consorte for helping to prepare the manuscript. The work is supported in part by DOE under contract No DE-AC04-76-00789 and by a Campus Laboratory Collaboration grant from the University of California.

References

[1] D'Andrea A, Del Sole R, Girlanda R and Quattropani A (eds) 1992 *Proc. Int. Conf. on Optics of Excitons in Confined Systems (Inst. Phys. Conf. Ser. 123)* (Bristol: Institute of Physics)
[2] Einevoll G T 1992 *Phys. Rev.* B **45** 3410
[3] See, for example, Bastard G 1988 *Wave Mechanics Applied to Semiconductor Heterostructures* (Les Ulis: Editions de Physique)
[4] Que W 1992 *Phys. Rev.* B **45** 11 036
[5] Barenco A and Dupertuis M A 1995 *Phys. Rev.* B **52** 2766
[6] Gotoh H, Ando H and Hiroshi K 1996 *Appl. Phys. Lett.* **68** 2132
[7] Bryant G W 1992 *Phys. Rev.* B **46** 1893
Bryant G W 1993 *Phys. Rev.* B **47** 1683
[8] Hohenberg P and Kohn W 1964 *Phys. Rev.* **136** B864
[9] Kohn W and Sham L J 1965 *Phys. Rev.* **140** A1133
[10] Fong C Y, Gallup R F, Nelson J S, Chang L L and Esaki L 1992 *Superlatt. Microstruct.* **11** 399
[11] Fong C Y, Nelson J S, Hemstreet L A, Gallup R F, Chang L L and Esaki L 1992 *Phys. Rev.* B **46** 9538
[12] Fong C Y, Zhong H, Klein B M and Nelson J S 1994 *Phys. Rev.* B **49** 7466
[13] Fong C Y, Klein B M and Nelson J S 1996 *Modelling Simul. Mater. Sci. Eng.* **4** 433
[14] Wang Y 1995 *Phys. Rev.* B **52** 2738
[15] Stoof T H and Bauer G E W 1995 *Phys. Rev.* B **52** 12 143
[16] Wunsche H J and Henneberger K 1979 *Phys. Status Solidi* b **91** 336
[17] Pfeiffer R S and Shore H B 1982 *Phys. Rev.* B **25** 3897
[18] Puls J, Wunsche H-J and Henneberger F 1996 *Chem. Phys.* **210** 235
[19] Nelson J S, Fong C Y and Batra I P 1987 *Appl. Phys. Lett.* **50** 1595
[20] Kohn W and Vashishta P 1983 *Theory of the Inhomogeneous Electron Gas* ed S Lundqvist and N H March (New York: Plenum) p 79
[21] Ceperley D M and Alder B J 1980 *Phys. Rev. Lett.* **45** 566
[22] Perdew J P and Zunger A 1981 *Phys. Rev.* B **23** 5048
[23] Woodward C, Min B I, Benedek R and Garner R 1989 *Phys. Rev.* B **39** 4853
[24] Schneider H, von Klitzing K and Ploog K 1989 *Superlatt. Microstruct.* **5** 383